Supporting Information

Cunning metal core: Efficiency/stability dilemma in metallated porphyrin based light-emitting electrochemical cells

Katharina T. Weber,[a†] Kostas Karikis,[b†] Michael D. Weber,[a] Pedro B. Coto,[c] Asterios Charisiadis,[b] Despina Charitaki,[b] Georgios Charalambidis,[b] Panagiotis Angaridis,[d] Athanassios G.Coutsolelos,[b*] and Rubén D. Costa[a*]

[a]*Department of Chemistry & Pharmacy, University of Erlangen-Nuremberg (FAU), Egerlandstr. 3, D-91058 Erlangen, Germany. E-mail: ruben.costa@fau.de*
[b] *Department of Chemistry, University of Crete, Laboratory of Bioinorganic Chemistry, Voutes Campus, P.O. Box 2208, 70013 Heraklion, Crete, Greece. E-mail: acoutsol@uoc.gr*
[c] *Chair of Solid State Theory, Physics Department, Friedrich-Alexander-Universität Erlangen-Nürnberg, Staudtstr. 7 / B2, 91058 Erlangen, Germany*
[d] *Department of Chemistry, Aristotle University of Thessaloniki, 54124 Thessaloniki, Greece*

1. Materials and techniques.

All chemicals and solvents were purchased from usual commercial sources and used as received, unless otherwise stated. Tetrahydrofuran (THF) was distilled from Na/benzophenone.

H_2-por[1], Zn-por[1] and Sn-por[2] were synthesized and purified according to literature procedures.

NMR spectra were recorded on Bruker AVANCE III-500 MHz and Bruker DPX-300 MHz spectrometers using solutions in deuterated solvents and the solvent peak was chosen as the internal standard.

High-resolution mass spectra (HRMS) were recorded on a Bruker UltrafleXtreme MALDI-TOF/TOF spectrometer, using trans-2-[3-(4-tert-Butylphenyl)-2-methyl-2-propenylidene] malononitrile as Matrix.

Single crystal X-ray crystallographic data were recorded on a STOE IPDS II diffractometer equipped with an image plate detector.

UV-vis absorption spectra were measured on a Shimadzu UV-1700 spectrophotometer using 10 mm path-length cuvettes with 2 x 10^{-5} M solution concentration. Emission spectra were measured on a JASCO FP-6500 fluorescence spectrophotometer equipped with a red sensitive WRE-343 photomultiplier tube (wavelength range 200-850 nm) with 2 x 10^{-5} M solution concentration. Emission lifetimes were determined by the time-correlated single-photon counting (TCSPC) technique using an Edinburgh Instruments mini-tau lifetime spectrophotometer equipped with an EPL 405 pulsed diode laser at 406.0 nm with a pulse width of 71.52 ps and a high-speed red-sensitive photomultiplier tube (H5773-04) as detector. Quantum yields were determined from corrected emission spectra following the standard methods[3] using 5,10,15,20-tetraphenylporphyrin (Φ = 11% in toluene),[4] as standard for Pd-por

and Pt-por and 5,10,15,20-tetraphenylporphyrinato zinc (Φ = 3% in toluene)[4] as standard for Zn-por and Sn-por.

Cyclic and square wave voltammetry experiments were carried out at room temperature using an AutoLab PGSTAT20 potentiostat and appropriate routines available in the operating software (GPES version 4.9). All measurements were carried out in freshly distilled and deoxygenated THF with a solute concentration of *ca*. 1.0 mM in the presence of tetrabutylammonium tetrafluoroborate (0.1 M) as supporting electrolyte, at a scan rate of 100 mV s^{-1}. A three-electrode cell setup was used with a platinum working electrode, a saturated calomel (SCE) reference electrode, and a platinum wire as counter electrode. In all measurements the ferrocene/ferrocenuim (Fc/Fc^+) redox was at 0.65 V versus SCEunder the above conditions. AFM assays were performed with VEECO DIMENSION 5000 with a NanoScope V probe head and the Gwyddion evaluation software.

2. Synthesis

Synthesis of Pt-por: $PtCl_2$ (125 mg, 0.47 mmol) was dissolved in benzonitrile (20mL) and refluxed for 1 h. H_2-Por (100 mg, 0.094 mmol) was added and the solution was further refluxed for 1h. After removal of the solvent under reduced pressure, CH_2Cl_2 (40 mL) was added and the mixture was washed with water (2x50 mL). The organic layer was dried over Na_2SO_4, filtered, concentrated, and the residue was purified by column chromatography on a silica gel (CH_2Cl_2 / hexane, 4:3 v/v) to obtain Pt-por (99 mg, 0.079 mmol, 84%) as an orange solid, mp >300 ^oC, ^1H NMR (500 MHz, $CDCl_3$): δ (ppm) 8.87 (s, 8H), 8.05 (d, J = 1.8 Hz, 8H), 7.78 (t, J = 1.8 Hz, 4H), 1.52 (s, 72H). ^{13}C NMR (75 MHz, $CDCl_3$): δ 148.8, 141.8, 141.1, 131.2, 129.4, 123.0, 121.1, 35.2, 31.9 ppm. HRMS (MALDI-TOF) calcd. for $C_{76}H_{93}N_4Pt$ $[M + H]^+$ 1256.7048, found 1256.7055. Anal. Calcd for $C_{76}H_{92}N_4Pt$: C, 72.64; H 7.38; N 4.46. Found: C, 72.69; H 7.47; N 4.31.

Synthesis of Pd-por: $PdCl_2$ (23 mg, 0.13 mmol) and H_2-por (70 mg, 0.065 mmol) were dissolved in benzonitrile (30 mL) and refluxed for 3 h. After removal of the solvents under reduced pressure, CH_2Cl_2 (40mL) was added and the mixture was washed with water (2x50 mL). The organic layer was dried over Na_2SO_4, filtered, concentrated, and the residue was purified by column chromatography on a silica gel (CH_2Cl_2 / hexane, 4:3 v/v) to obtain Pd-por (75 mg, 0.064 mmol, 99%) as an orange solid, mp >300 ^oC, ^1H NMR (500 MHz, $CDCl_3$): δ (ppm) 8.87 (s, 8H), 8.04 (d, J = 1.7 Hz, 8H), 7.77 (t, J = 1.7 Hz, 4H), 1.51 (s, 72H). ^{13}C NMR (75 MHz, $CDCl_3$): δ 148.8, 141.8, 141.1, 131.2, 129.4, 123.0, 121.1, 35.2, 31.9 ppm. HRMS (MALDI-TOF) calcd. for $C_{76}H_{92}N_4Pd$ $[M]^+$ 1166.6357, found 1166.6347. Anal. Calcd for $C_{76}H_{92}N_4Pd$: C, 78.15; H 7.94; N 4.80. Found: C, 78.22; H 7.88; N 4.85.

3. Device fabrication and analysis

Double layer LECs were fabricated as follows. ITO coated glass plates were patterned by conventional photolithography (Naranjo Substrates). The substrates were cleaned by using sequential ultrasonic baths, namely in water-soap, water, ethanol, and propan-2-ol solvents. After drying, the substrates were placed in a UV–ozone cleaner (Jetlight 42-220) for 8 min. An 40 nm layer of PEDOT:PSS was spin-coatedonto the ITO-glass substrate to increase the device preparation yield.The PEDOT:PSS was diluted with propan-2-ol in a ratio of 2:1 and the substrate was spun for 35 s at 2000 rpm. The luminescent layer consists of a mixture of the Sn-por, Zn-por, Pt-por with the ionic polyelectrolyte in a mass ratio 1:0.15:0.06 (porphyrin:TMPE:LiTf). The active layer was deposited by means of spin coating (700 rpm spinning velocity) reaching a thickness of 110-130 nm. These conditions resulted in homogenous thin films with a roughness less than 5 %, having no apparent optical defects. The latter was determined using the profilometer DektakxT from Bruker. The only exception is the Pd-por compound. In this case, the morphology did not enhance after several trials changing i) the concentration of the compound from 7.5–10 mg/ml, ii) the solvents – *i.e.*, THF, chlorobenzene, and toluene, iii) the mass ratios with the matrix, and iv) the deposition technique, namely spin-coating at 800, 1200, 3000 rpm under air and N_2 conditions, as well as doctor-blading at different substrate distances (850- 1000 μm), speeds (5-15 mm/s), and temperatures (30-50 °C).

Once the active layer was deposited, the samples were transferred into an inert atmosphere glovebox (<0.1 ppm O_2 and H_2O, Innovative Technology). Aluminum cathode electrode (90 nm) was thermally evaporated using a shadow mask under high vacuum (<1 x 10^{-6} mbar) using an Angstrom Covap evaporator integrated into the inert atmosphere glovebox. Time dependence of luminance, voltage, and current was measured by applying constant and/or pulsed voltage and current by monitoring the desired parameters simultaneously by using Avantes spectrophotometer (Avaspec-ULS2048L-USB2) in conjunction with a calibrated integrated sphere Avasphere 30-Irrad and Botest OLT OLED Lifetime-Test System. Electroluminescence spectra were recorded using the above-mentioned spectrophotometer. The devices were analyzed by means of long-term measurements with driving schemes based on an average pulsed current of 7.5mA with a block-wave at 1000 Hz and a duty cycle of 50 %.Electrochemical impedance spectroscopic assays (EIS) were carried out with a potentiostat/galvanostat (Metrohm μAutolabIII) equipped with a frequency response analyzer module (FRA2). Measurements were performed at the applied voltage range from 0 to 4 V and fitted with the Nova software using the circuit model shown in Figure S14. The AC signal amplitude was set to 10 mV, modulated in a frequency range from 10 to 1 MHz. The Nova 1.11 software was used to obtain the parameters from the equivalent circuit. With this data at hand, the resistance of the intrinsic non-doped

region (R_i) was directly obtained. The film conductivity (σ) was determined at applied voltage of 0 V with the following equation:

$$\sigma = \frac{d}{AR_i}$$

where d is the thickness of the layer, A is the area of the electrodes, and R_i is the resistance of the active layer.

4. Theoretical description

To investigate the electronic spectra of Sn-por, we have employed a theoretical approach that combines DFT calculations with linear-response time-dependent density functional theory (TD-DFT). Specifically, the equilibrium structures of Sn-por were optimized using the B3LYP exchange-correlation functional,[5-10] employing the def2-TZVP basis set.[11] The core electrons of Sn were described using the Stuttgart ecp-28-mdf pseudopotential.[12] Symmetry was not imposed in the optimization of the ground state molecular structure. Vertical excitation energies (ΔE) and oscillator strengths (f) of the electronic excited states of interest (the Soret and Q bands) were obtained using TD-DFT, employing the B3LYP exchange-correlation functional, the def2-TZVP basis set and the Stuttgart ecp-28-mdf pseudopotential for the description of the core electrons of Sn. To investigate the effect that relaxation has in the energy difference between S_1 and T_1, we have obtained the equilibrium structures of these states using the same level of theory. To avoid root-flipping problems during the relaxation, the calculations were carried out using D_{2h} symmetry. The results show a S_1-T_1 adiabatic energy difference of ~0.8 eV, in line with the vertical energy difference found at the ground state equilibrium structure. All the calculations were carried out using TURBOMOLE.[13]

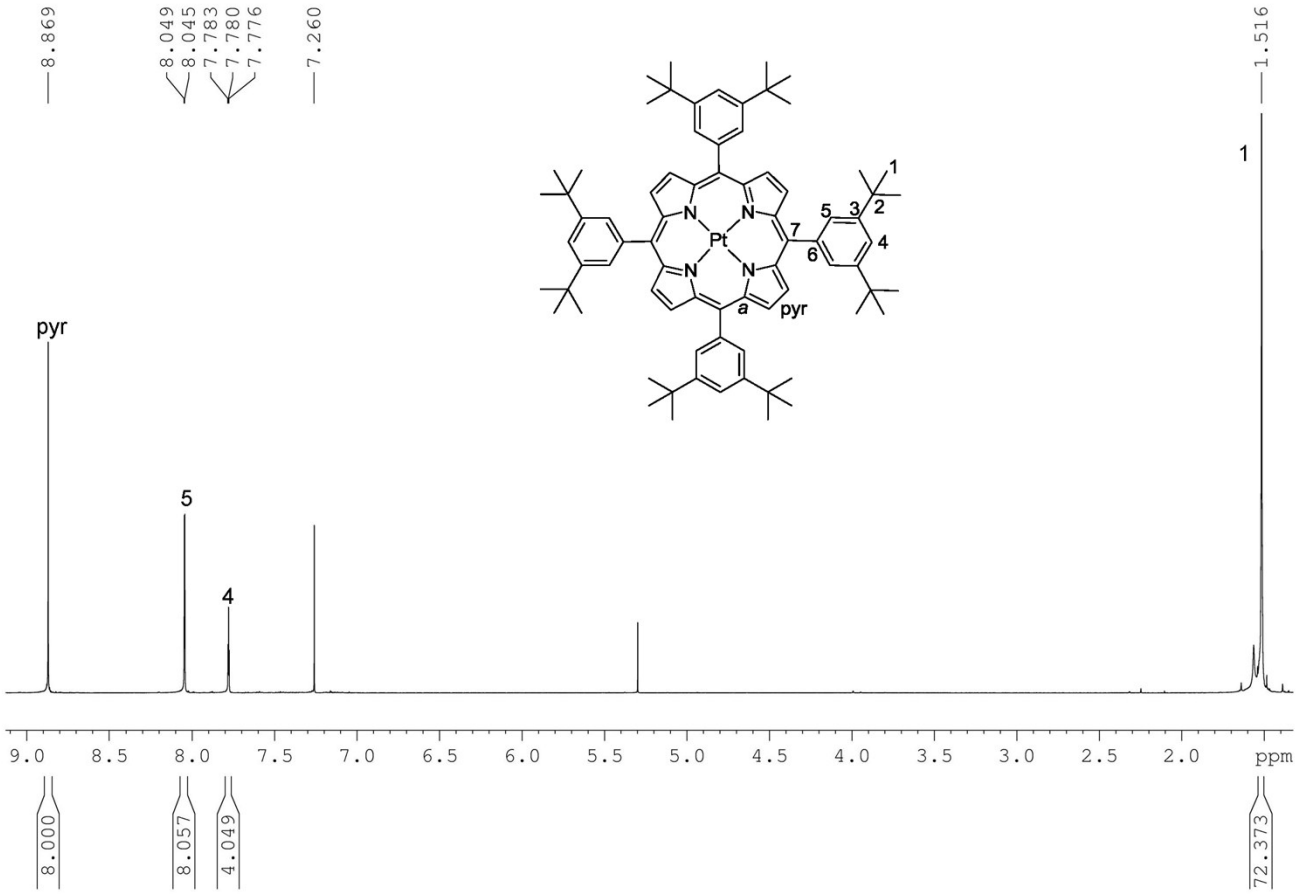

Figure S1. ^{1}H NMR spectrum of Pt-por in $CDCl_3$.

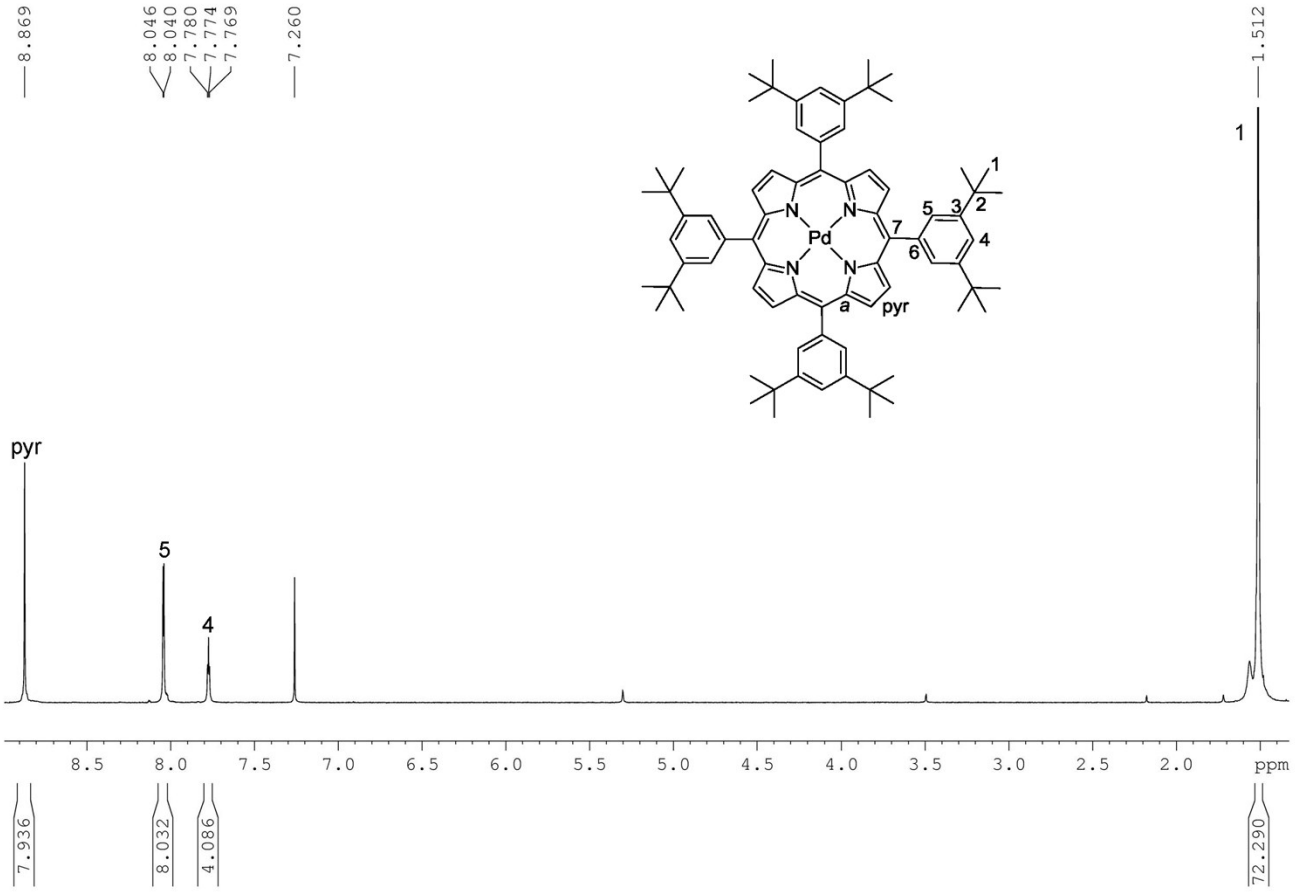

Figure S2. ^{1}H NMR spectrum of Pd-por in $CDCl_3$.

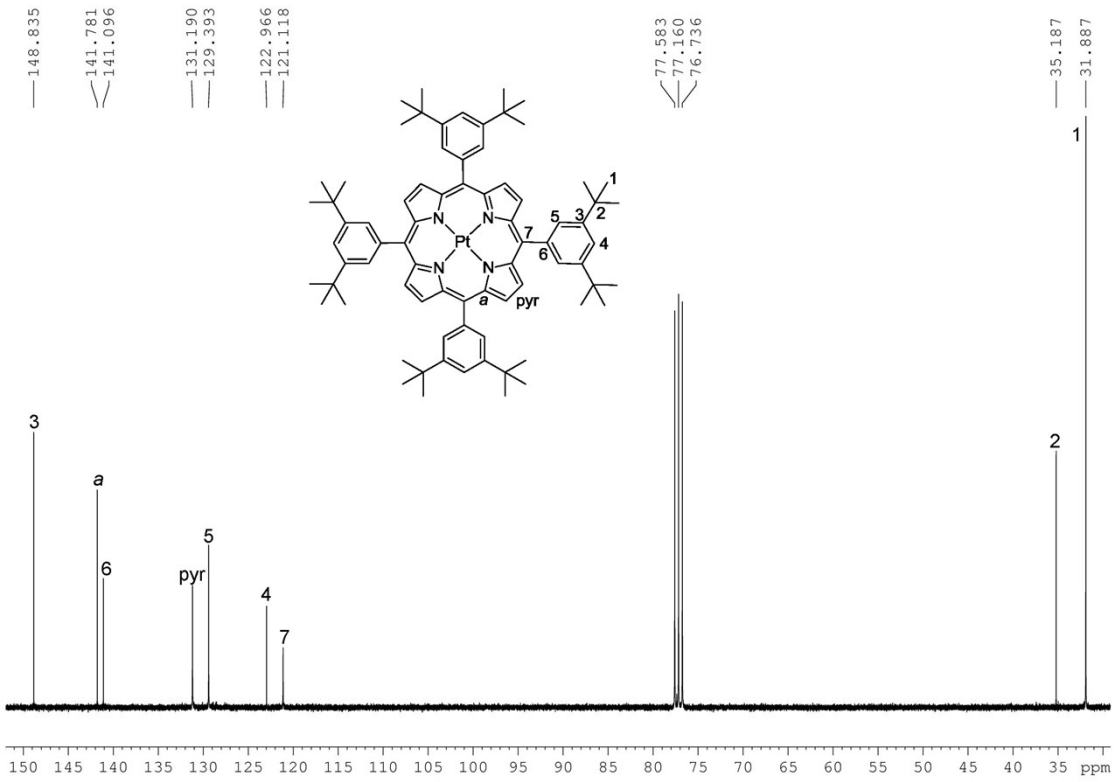

Figure S3. ^{13}C NMR spectrum of Pt-por in $CDCl_3$.

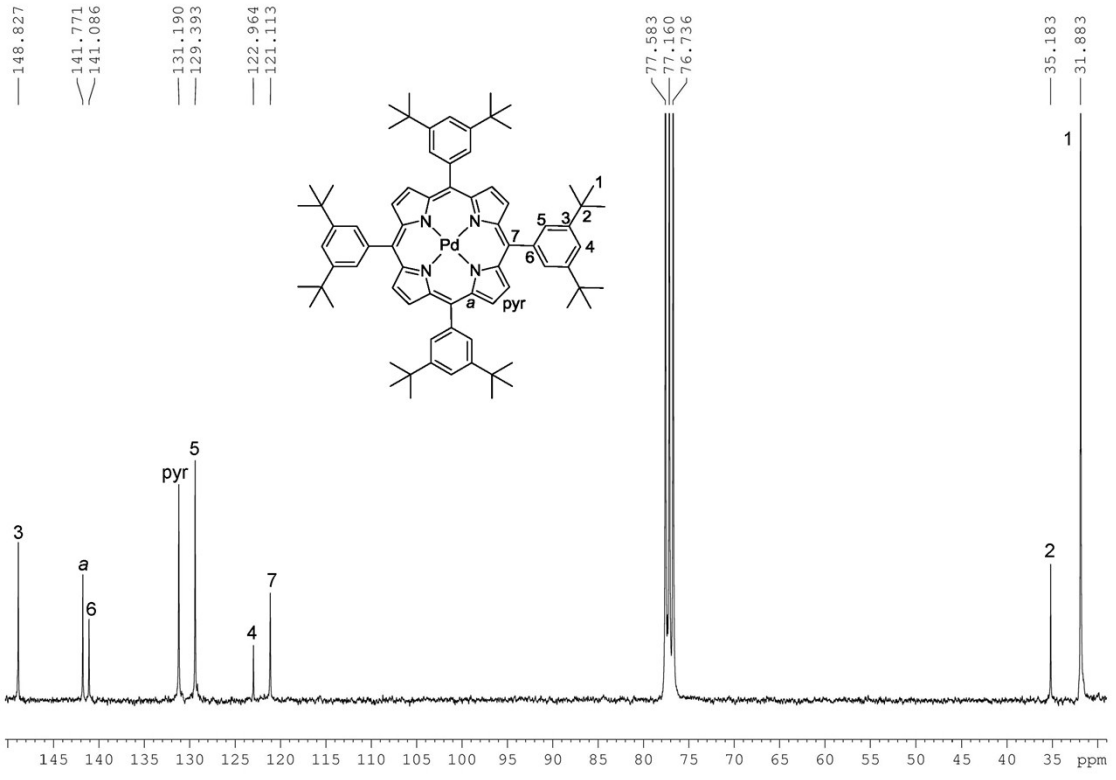

Figure S4. ^{13}C NMR spectrum of Pt-por in $CDCl_3$.

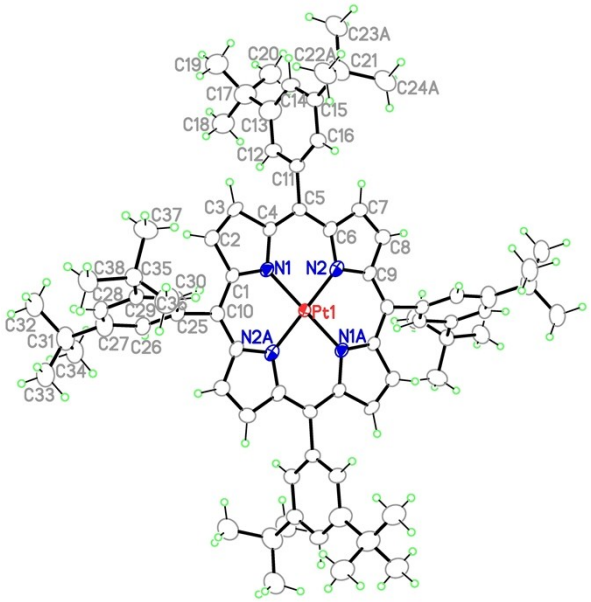

Figure S5. ORTEP representation of X-ray crystal structure of Pt-por with all non-hydrogen atoms represented by thermal ellipsoids at the 35% probability level. The solvent molecule of crystallization (n-C_7H_{16}) is omitted for clarity.

Table S1. Crystal data and structure refinement for Pt-por·C_7H_{16}.

Empirical formula	C83 H108 N4 Pt	
Formula weight	1356.82	
Temperature	293(2) K	
Wavelength	0.71073 Å	
Crystal system	Triclinic	
Space group	P -1	
Unit cell dimensions	a = 9.5314(19) Å	α= 89.65(3)°.
	b = 14.518(3) Å	β= 82.60(3)°.
	c = 15.621(3) Å	γ = 74.32(3)°.
Volume	2062.9(8) $Å^3$	
Z	1	
Density (calculated)	1.092 Mg/m^3	
Absorption coefficient	1.740 mm^{-1}	
F(000)	712	
Crystal size	0.45 x 0.35 x 0.25 mm^3	
Theta range for data collection	1.934 to 24.997°.	
Index ranges	-11<=h<=11, -17<=k<=17, -18<=l<=18	
Reflections collected	7247	
Independent reflections	7247 [R(int) = 0.0838]	

Completeness to theta = 24.997°	99.6 %
Absorption correction	Numerical
Max. and min. transmission	0.6751 and 0.4817
Refinement method	Full-matrix least-squares on F^2
Data / restraints / parameters	7247 / 31 / 315
Goodness-of-fit on F^2	1.384
Final R indices [I>2sigma(I)]	R1 = 0.0796, wR2 = 0.1865
R indices (all data)	R1 = 0.0863, wR2 = 0.1963
Largest diff. peak and hole	3.526 and -4.704 e.$Å^{-3}$

Table S2. Atomic coordinates ($\times 10^4$) and equivalent isotropic displacement parameters ($Å^2 \times 10^3$) for Pt-por. U(eq) is defined as one third of the trace of the orthogonalized U^{ij} tensor.

	x	y	z	U(eq)
Pt(1)	0	5000	5000	30(1)
N(1)	157(8)	4604(5)	3746(4)	33(1)
N(2)	1763(8)	3950(5)	5141(5)	39(1)
C(1)	-747(9)	4999(6)	3162(5)	33(1)
C(2)	-318(11)	4462(7)	2360(7)	49(2)
C(3)	881(11)	3748(7)	2450(6)	48(2)
C(4)	1196(9)	3817(6)	3331(5)	34(1)
C(5)	2366(9)	3197(6)	3665(6)	37(2)
C(6)	2595(10)	3267(6)	4527(6)	39(1)
C(7)	3770(11)	2597(7)	4907(7)	47(2)
C(8)	3640(11)	2878(7)	5736(7)	46(2)
C(9)	2413(10)	3699(6)	5902(6)	39(1)
C(10)	-1983(10)	5812(6)	3322(6)	37(2)
C(11)	3381(6)	2406(4)	3088(4)	39(2)
C(12)	2970(6)	1573(4)	2959(4)	43(2)
C(13)	3890(7)	841(4)	2417(5)	82(2)
C(14)	5219(7)	941(4)	2003(4)	51(3)
C(15)	5630(5)	1774(5)	2132(4)	48(2)
C(16)	4710(6)	2506(4)	2674(4)	44(2)
C(17)	3458(16)	-102(9)	2281(10)	82(2)
C(18)	1950(16)	-84(9)	2694(10)	82(2)
C(19)	3546(16)	-315(9)	1309(10)	82(2)
C(20)	4557(16)	-934(9)	2628(10)	82(2)
C(21)	7102(14)	1891(12)	1672(10)	85(3)
C(22A)	6820(20)	2696(18)	1066(17)	85(3)
C(23A)	8080(20)	969(18)	1193(17)	85(3)
C(24A)	8050(20)	2110(20)	2365(15)	85(3)
C(22B)	7400(30)	1500(30)	710(19)	85(3)
C(23B)	8310(30)	1460(20)	2120(20)	85(3)
C(24B)	7000(30)	3020(20)	1570(20)	85(3)
C(25)	-2807(6)	6144(5)	2568(3)	40(2)
C(26)	-4180(6)	5986(5)	2556(3)	43(2)
C(27)	-4927(6)	6247(5)	1846(4)	73(2)
C(28)	-4301(6)	6665(5)	1148(3)	42(2)

C(29)	-2929(6)	6822(4)	1160(3)	39(2)
C(30)	-2182(5)	6562(5)	1870(4)	43(2)
C(31)	-6466(14)	6079(10)	1815(9)	73(2)
C(32)	-6446(14)	5471(10)	1034(9)	73(2)
C(33)	-7591(14)	7047(9)	1750(9)	73(2)
C(34)	-7003(14)	5590(10)	2612(9)	73(2)
C(35)	-2158(11)	7253(7)	372(6)	46(2)
C(36)	-1659(16)	8110(9)	679(8)	73(4)
C(37)	-802(13)	6473(10)	-29(8)	71(3)
C(38)	-3151(13)	7593(9)	-321(7)	62(3)
C(1S)	6720(30)	3770(20)	4453(19)	80(7)
C(2S)	7600(40)	3150(30)	4960(30)	116(12)
C(3S)	8720(30)	2500(20)	4922(19)	79(7)
C(4S)	9640(40)	1880(30)	5520(20)	102(10)
C(5S)	10800(30)	1270(20)	5460(20)	87(8)
C(6S)	11680(40)	720(20)	6060(20)	101(10)
C(7S)	12890(50)	50(30)	5800(30)	131(14)

Table S3. Bond lengths [Å] and angles [°] for Pt-por.

Pt(1)-N(2)	1.975(8)
Pt(1)-N(2)#1	1.976(8)
Pt(1)-N(1)	2.021(7)
Pt(1)-N(1)#1	2.021(7)
N(1)-C(4)	1.392(11)
N(1)-C(1)	1.354(11)
N(2)-C(6)	1.386(12)
N(2)-C(9)	1.412(12)
C(1)-C(10)	1.421(12)
C(1)-C(2)	1.432(13)
C(2)-C(3)	1.341(14)
C(2)-H(2A)	0.9300
C(3)-C(4)	1.456(12)
C(3)-H(3A)	0.9300
C(4)-C(5)	1.389(12)
C(5)-C(6)	1.401(13)
C(5)-C(11)	1.502(9)
C(6)-C(7)	1.459(14)
C(7)-C(8)	1.340(14)
C(7)-H(7A)	0.9300
C(8)-C(9)	1.424(13)
C(8)-H(8A)	0.9300
C(9)-C(10)#1	1.367(13)
C(10)-C(9)#1	1.367(13)
C(10)-C(25)	1.504(10)
C(11)-C(12)	1.3900
C(11)-C(16)	1.3900
C(12)-C(13)	1.3900
C(12)-H(12A)	0.9300
C(13)-C(14)	1.3900
C(13)-C(17)	1.556(13)
C(14)-C(15)	1.3900
C(14)-H(14A)	0.9300
C(15)-C(16)	1.3900
C(15)-C(21)	1.544(13)
C(16)-H(16A)	0.9300
C(17)-C(18)	1.491(19)

C(17)-C(19)	1.54(2)
C(17)-C(20)	1.52(2)
C(18)-H(18A)	0.9600
C(18)-H(18B)	0.9600
C(18)-H(18C)	0.9600
C(19)-H(19A)	0.9600
C(19)-H(19B)	0.9600
C(19)-H(19C)	0.9600
C(20)-H(20A)	0.9600
C(20)-H(20B)	0.9600
C(20)-H(20C)	0.9600
C(21)-C(23B)	1.42(3)
C(21)-C(22A)	1.49(3)
C(21)-C(22B)	1.57(3)
C(21)-C(23A)	1.54(3)
C(21)-C(24A)	1.58(3)
C(21)-C(24B)	1.63(3)
C(22A)-H(22A)	0.9600
C(22A)-H(22B)	0.9600
C(22A)-H(22C)	0.9600
C(23A)-H(23A)	0.9600
C(23A)-H(23B)	0.9600
C(23A)-H(23C)	0.9600
C(24A)-H(24A)	0.9600
C(24A)-H(24B)	0.9600
C(24A)-H(24C)	0.9600
C(22B)-H(22D)	0.9600
C(22B)-H(22E)	0.9600
C(22B)-H(22F)	0.9600
C(23B)-H(23D)	0.9600
C(23B)-H(23E)	0.9600
C(23B)-H(23F)	0.9600
C(24B)-H(24D)	0.9600
C(24B)-H(24E)	0.9600
C(24B)-H(24F)	0.9600
C(25)-C(26)	1.3900
C(25)-C(30)	1.3900
C(26)-C(27)	1.3900
C(26)-H(26A)	0.9300

C(27)-C(28)	1.3900
C(27)-C(31)	1.557(13)
C(28)-C(29)	1.3900
C(28)-H(28A)	0.9300
C(29)-C(30)	1.3900
C(29)-C(35)	1.566(10)
C(30)-H(30A)	0.9300
C(31)-C(32)	1.506(18)
C(31)-C(34)	1.529(19)
C(31)-C(33)	1.532(18)
C(32)-H(32A)	0.9600
C(32)-H(32B)	0.9600
C(32)-H(32C)	0.9600
C(33)-H(33A)	0.9600
C(33)-H(33B)	0.9600
C(33)-H(33C)	0.9600
C(34)-H(34A)	0.9600
C(34)-H(34B)	0.9600
C(34)-H(34C)	0.9600
C(35)-C(36)	1.546(16)
C(35)-C(37)	1.534(15)
C(35)-C(38)	1.520(14)
C(36)-H(36A)	0.9600
C(36)-H(36B)	0.9600
C(36)-H(36C)	0.9600
C(37)-H(37A)	0.9600
C(37)-H(37B)	0.9600
C(37)-H(37C)	0.9600
C(38)-H(38A)	0.9600
C(38)-H(38B)	0.9600
C(38)-H(38C)	0.9600
C(1S)-C(2S)	1.37(4)
C(1S)-H(1S1)	0.9600
C(1S)-H(1S2)	0.9600
C(1S)-H(1S3)	0.9600
C(2S)-C(3S)	1.22(4)
C(2S)-H(2S1)	0.9700
C(2S)-H(2S2)	0.9700
C(3S)-C(4S)	1.49(4)

C(3S)-H(3S1)	0.9700
C(3S)-H(3S2)	0.9700
C(4S)-C(5S)	1.21(4)
C(4S)-H(4S1)	0.9700
C(4S)-H(4S2)	0.9700
C(5S)-C(6S)	1.43(4)
C(5S)-H(5S1)	0.9700
C(5S)-H(5S2)	0.9700
C(6S)-C(7S)	1.30(5)
C(6S)-H(6S1)	0.9700
C(6S)-H(6S2)	0.9700
C(7S)-H(7S1)	0.9600
C(7S)-H(7S2)	0.9600
C(7S)-H(7S3)	0.9600
N(2)-Pt(1)-N(2)#1	180.0
N(2)-Pt(1)-N(1)	90.4(3)
N(2)#1-Pt(1)-N(1)	89.6(3)
N(2)-Pt(1)-N(1)#1	89.6(3)
N(2)#1-Pt(1)-N(1)#1	90.4(3)
N(1)-Pt(1)-N(1)#1	180.0(4)
C(4)-N(1)-C(1)	106.6(7)
C(4)-N(1)-Pt(1)	125.4(6)
C(1)-N(1)-Pt(1)	127.9(6)
C(6)-N(2)-C(9)	104.5(7)
C(6)-N(2)-Pt(1)	127.8(6)
C(9)-N(2)-Pt(1)	127.6(6)
C(10)-C(1)-N(1)	125.3(8)
C(10)-C(1)-C(2)	124.2(8)
N(1)-C(1)-C(2)	110.5(8)
C(3)-C(2)-C(1)	107.5(9)
C(3)-C(2)-H(2A)	126.3
C(1)-C(2)-H(2A)	126.3
C(2)-C(3)-C(4)	107.2(8)
C(2)-C(3)-H(3A)	126.4
C(4)-C(3)-H(3A)	126.4
C(5)-C(4)-N(1)	127.7(8)
C(5)-C(4)-C(3)	124.0(8)
N(1)-C(4)-C(3)	108.2(8)
C(4)-C(5)-C(6)	122.1(8)

C(4)-C(5)-C(11)	118.6(8)
C(6)-C(5)-C(11)	119.3(8)
N(2)-C(6)-C(5)	126.5(9)
N(2)-C(6)-C(7)	110.2(8)
C(5)-C(6)-C(7)	123.3(9)
C(8)-C(7)-C(6)	106.7(8)
C(8)-C(7)-H(7A)	126.7
C(6)-C(7)-H(7A)	126.7
C(7)-C(8)-C(9)	108.6(9)
C(7)-C(8)-H(8A)	125.7
C(9)-C(8)-H(8A)	125.7
N(2)-C(9)-C(10)#1	125.7(8)
N(2)-C(9)-C(8)	110.0(8)
C(10)#1-C(9)-C(8)	124.3(9)
C(1)-C(10)-C(9)#1	123.8(8)
C(1)-C(10)-C(25)	116.1(7)
C(9)#1-C(10)-C(25)	120.1(8)
C(12)-C(11)-C(16)	120.0
C(12)-C(11)-C(5)	119.4(5)
C(16)-C(11)-C(5)	120.6(5)
C(11)-C(12)-C(13)	120.0
C(11)-C(12)-H(12A)	120.0
C(13)-C(12)-H(12A)	120.0
C(12)-C(13)-C(14)	120.0
C(12)-C(13)-C(17)	120.5(7)
C(14)-C(13)-C(17)	119.5(7)
C(15)-C(14)-C(13)	120.0
C(15)-C(14)-H(14A)	120.0
C(13)-C(14)-H(14A)	120.0
C(14)-C(15)-C(16)	120.0
C(14)-C(15)-C(21)	120.3(7)
C(16)-C(15)-C(21)	119.7(7)
C(15)-C(16)-C(11)	120.0
C(15)-C(16)-H(16A)	120.0
C(11)-C(16)-H(16A)	120.0
C(13)-C(17)-C(18)	114.1(10)
C(13)-C(17)-C(19)	109.7(11)
C(18)-C(17)-C(19)	107.8(12)
C(13)-C(17)-C(20)	109.7(11)

C(18)-C(17)-C(20)	108.8(12)
C(19)-C(17)-C(20)	106.6(11)
C(17)-C(18)-H(18A)	109.5
C(17)-C(18)-H(18B)	109.5
H(18A)-C(18)-H(18B)	109.5
C(17)-C(18)-H(18C)	109.5
H(18A)-C(18)-H(18C)	109.5
H(18B)-C(18)-H(18C)	109.5
C(17)-C(19)-H(19A)	109.5
C(17)-C(19)-H(19B)	109.5
H(19A)-C(19)-H(19B)	109.5
C(17)-C(19)-H(19C)	109.5
H(19A)-C(19)-H(19C)	109.5
H(19B)-C(19)-H(19C)	109.5
C(17)-C(20)-H(20A)	109.5
C(17)-C(20)-H(20B)	109.5
H(20A)-C(20)-H(20B)	109.5
C(17)-C(20)-H(20C)	109.5
H(20A)-C(20)-H(20C)	109.5
H(20B)-C(20)-H(20C)	109.5
C(23B)-C(21)-C(15)	112.6(16)
C(22A)-C(21)-C(15)	109.8(13)
C(23B)-C(21)-C(22B)	110.6(18)
C(15)-C(21)-C(22B)	111.1(14)
C(22A)-C(21)-C(23A)	110.4(16)
C(15)-C(21)-C(23A)	113.2(13)
C(22A)-C(21)-C(24A)	109.5(17)
C(15)-C(21)-C(24A)	109.5(13)
C(23A)-C(21)-C(24A)	104.3(15)
C(23B)-C(21)-C(24B)	109.3(18)
C(15)-C(21)-C(24B)	109.7(13)
C(22B)-C(21)-C(24B)	103.1(19)
C(21)-C(22A)-H(22A)	109.5
C(21)-C(22A)-H(22B)	109.5
H(22A)-C(22A)-H(22B)	109.5
C(21)-C(22A)-H(22C)	109.5
H(22A)-C(22A)-H(22C)	109.5
H(22B)-C(22A)-H(22C)	109.5
C(21)-C(23A)-H(23A)	109.5

C(21)-C(23A)-H(23B)	109.5
H(23A)-C(23A)-H(23B)	109.5
C(21)-C(23A)-H(23C)	109.5
H(23A)-C(23A)-H(23C)	109.5
H(23B)-C(23A)-H(23C)	109.5
C(21)-C(24A)-H(24A)	109.5
C(21)-C(24A)-H(24B)	109.5
H(24A)-C(24A)-H(24B)	109.5
C(21)-C(24A)-H(24C)	109.5
H(24A)-C(24A)-H(24C)	109.5
H(24B)-C(24A)-H(24C)	109.5
C(21)-C(22B)-H(22D)	109.5
C(21)-C(22B)-H(22E)	109.5
H(22D)-C(22B)-H(22E)	109.5
C(21)-C(22B)-H(22F)	109.5
H(22D)-C(22B)-H(22F)	109.5
H(22E)-C(22B)-H(22F)	109.5
C(21)-C(23B)-H(23D)	109.5
C(21)-C(23B)-H(23E)	109.5
H(23D)-C(23B)-H(23E)	109.5
C(21)-C(23B)-H(23F)	109.5
H(23D)-C(23B)-H(23F)	109.5
H(23E)-C(23B)-H(23F)	109.5
C(21)-C(24B)-H(24D)	109.5
C(21)-C(24B)-H(24E)	109.5
H(24D)-C(24B)-H(24E)	109.5
C(21)-C(24B)-H(24F)	109.5
H(24D)-C(24B)-H(24F)	109.5
H(24E)-C(24B)-H(24F)	109.5
C(26)-C(25)-C(30)	120.0
C(26)-C(25)-C(10)	119.2(5)
C(30)-C(25)-C(10)	120.8(5)
C(25)-C(26)-C(27)	120.0
C(25)-C(26)-H(26A)	120.0
C(27)-C(26)-H(26A)	120.0
C(28)-C(27)-C(26)	120.0
C(28)-C(27)-C(31)	118.9(6)
C(26)-C(27)-C(31)	121.1(6)
C(27)-C(28)-C(29)	120.0

C(27)-C(28)-H(28A)	120.0
C(29)-C(28)-H(28A)	120.0
C(30)-C(29)-C(28)	120.0
C(30)-C(29)-C(35)	118.4(5)
C(28)-C(29)-C(35)	121.6(5)
C(29)-C(30)-C(25)	120.0
C(29)-C(30)-H(30A)	120.0
C(25)-C(30)-H(30A)	120.0
C(27)-C(31)-C(32)	110.6(10)
C(27)-C(31)-C(34)	113.4(10)
C(32)-C(31)-C(34)	107.7(11)
C(27)-C(31)-C(33)	108.9(9)
C(32)-C(31)-C(33)	108.1(11)
C(34)-C(31)-C(33)	107.9(11)
C(31)-C(32)-H(32A)	109.5
C(31)-C(32)-H(32B)	109.5
H(32A)-C(32)-H(32B)	109.5
C(31)-C(32)-H(32C)	109.5
H(32A)-C(32)-H(32C)	109.5
H(32B)-C(32)-H(32C)	109.5
C(31)-C(33)-H(33A)	109.5
C(31)-C(33)-H(33B)	109.5
H(33A)-C(33)-H(33B)	109.5
C(31)-C(33)-H(33C)	109.5
H(33A)-C(33)-H(33C)	109.5
H(33B)-C(33)-H(33C)	109.5
C(31)-C(34)-H(34A)	109.5
C(31)-C(34)-H(34B)	109.5
H(34A)-C(34)-H(34B)	109.5
C(31)-C(34)-H(34C)	109.5
H(34A)-C(34)-H(34C)	109.5
H(34B)-C(34)-H(34C)	109.5
C(36)-C(35)-C(37)	109.0(10)
C(36)-C(35)-C(29)	109.9(8)
C(37)-C(35)-C(29)	108.1(8)
C(36)-C(35)-C(38)	108.5(9)
C(37)-C(35)-C(38)	108.5(9)
C(29)-C(35)-C(38)	112.8(8)
C(35)-C(36)-H(36A)	109.5

C(35)-C(36)-H(36B)	109.5
H(36A)-C(36)-H(36B)	109.5
C(35)-C(36)-H(36C)	109.5
H(36A)-C(36)-H(36C)	109.5
H(36B)-C(36)-H(36C)	109.5
C(35)-C(37)-H(37A)	109.5
C(35)-C(37)-H(37B)	109.5
H(37A)-C(37)-H(37B)	109.5
C(35)-C(37)-H(37C)	109.5
H(37A)-C(37)-H(37C)	109.5
H(37B)-C(37)-H(37C)	109.5
C(35)-C(38)-H(38A)	109.5
C(35)-C(38)-H(38B)	109.5
H(38A)-C(38)-H(38B)	109.5
C(35)-C(38)-H(38C)	109.5
H(38A)-C(38)-H(38C)	109.5
H(38B)-C(38)-H(38C)	109.5
C(2S)-C(1S)-H(1S1)	109.5
C(2S)-C(1S)-H(1S2)	109.5
H(1S1)-C(1S)-H(1S2)	109.5
C(2S)-C(1S)-H(1S3)	109.5
H(1S1)-C(1S)-H(1S3)	109.5
H(1S2)-C(1S)-H(1S3)	109.5
C(3S)-C(2S)-C(1S)	143(4)
C(3S)-C(2S)-H(2S1)	101.3
C(1S)-C(2S)-H(2S1)	101.3
C(3S)-C(2S)-H(2S2)	101.3
C(1S)-C(2S)-H(2S2)	101.3
H(2S1)-C(2S)-H(2S2)	104.6
C(2S)-C(3S)-C(4S)	139(3)
C(2S)-C(3S)-H(3S1)	102.3
C(4S)-C(3S)-H(3S1)	102.3
C(2S)-C(3S)-H(3S2)	102.3
C(4S)-C(3S)-H(3S2)	102.3
H(3S1)-C(3S)-H(3S2)	104.9
C(5S)-C(4S)-C(3S)	137(4)
C(5S)-C(4S)-H(4S1)	102.9
C(3S)-C(4S)-H(4S1)	102.9
C(5S)-C(4S)-H(4S2)	102.9

C(3S)-C(4S)-H(4S2)	102.9
H(4S1)-C(4S)-H(4S2)	105.1
C(4S)-C(5S)-C(6S)	135(3)
C(4S)-C(5S)-H(5S1)	103.3
C(6S)-C(5S)-H(5S1)	103.3
C(4S)-C(5S)-H(5S2)	103.3
C(6S)-C(5S)-H(5S2)	103.3
H(5S1)-C(5S)-H(5S2)	105.2
C(7S)-C(6S)-C(5S)	122(4)
C(7S)-C(6S)-H(6S1)	106.7
C(5S)-C(6S)-H(6S1)	106.7
C(7S)-C(6S)-H(6S2)	106.7
C(5S)-C(6S)-H(6S2)	106.7
H(6S1)-C(6S)-H(6S2)	106.6
C(6S)-C(7S)-H(7S1)	109.5
C(6S)-C(7S)-H(7S2)	109.5
H(7S1)-C(7S)-H(7S2)	109.5
C(6S)-C(7S)-H(7S3)	109.5
H(7S1)-C(7S)-H(7S3)	109.5
H(7S2)-C(7S)-H(7S3)	109.5

Symmetry transformations used to generate equivalent atoms:

#1 -x,-y+1,-z+1

Table S4. Anisotropic displacement parameters ($Å^2 \times 10^3$) for Pt-por. The anisotropic displacement factor exponent takes the form: $-2\pi^2[h^2a^{*2}U^{11} + ... + 2 h k a^* b^* U^{12}]$

	U^{11}	U^{22}	U^{33}	U^{23}	U^{13}	U^{12}
Pt(1)	28(1)	34(1)	28(1)	-3(1)	-5(1)	-9(1)
N(1)	37(3)	40(3)	24(2)	-1(2)	-6(2)	-12(2)
N(2)	46(3)	40(3)	36(3)	-4(2)	-9(2)	-17(2)
C(1)	37(3)	40(3)	25(2)	0(2)	-6(2)	-12(2)
C(2)	47(6)	56(6)	43(6)	-11(5)	-13(5)	-9(5)
C(3)	55(6)	53(6)	35(5)	-18(4)	-9(5)	-9(5)
C(4)	37(3)	40(3)	25(2)	-2(2)	-5(2)	-12(2)
C(5)	30(4)	40(5)	39(5)	-5(4)	-2(4)	-6(4)
C(6)	46(3)	41(3)	36(3)	-4(2)	-9(2)	-17(2)
C(7)	40(5)	45(6)	50(6)	-8(5)	-4(5)	-4(4)
C(8)	49(6)	41(5)	44(6)	-1(4)	-15(5)	0(4)
C(9)	45(3)	40(3)	35(3)	-4(2)	-10(2)	-16(2)
C(10)	35(5)	35(5)	43(5)	3(4)	-8(4)	-12(4)
C(11)	39(5)	37(5)	35(5)	-4(4)	-4(4)	-4(4)
C(12)	41(5)	42(5)	45(6)	-6(4)	5(4)	-15(4)
C(13)	85(4)	60(3)	101(5)	-15(3)	-3(4)	-25(3)
C(14)	48(6)	51(6)	47(6)	-13(5)	6(5)	-10(5)
C(15)	40(5)	61(6)	42(6)	-7(5)	6(4)	-14(5)
C(16)	37(5)	51(6)	42(6)	-4(4)	2(4)	-14(4)
C(17)	85(4)	60(3)	101(5)	-15(3)	-3(4)	-25(3)
C(18)	85(4)	60(3)	101(5)	-15(3)	-3(4)	-25(3)
C(19)	85(4)	60(3)	101(5)	-15(3)	-3(4)	-25(3)
C(20)	85(4)	60(3)	101(5)	-15(3)	-3(4)	-25(3)
C(21)	48(4)	118(8)	88(7)	-8(5)	12(4)	-31(5)
C(22A)	48(4)	118(8)	88(7)	-8(5)	12(4)	-31(5)
C(23A)	48(4)	118(8)	88(7)	-8(5)	12(4)	-31(5)
C(24A)	48(4)	118(8)	88(7)	-8(5)	12(4)	-31(5)
C(22B)	48(4)	118(8)	88(7)	-8(5)	12(4)	-31(5)
C(23B)	48(4)	118(8)	88(7)	-8(5)	12(4)	-31(5)
C(24B)	48(4)	118(8)	88(7)	-8(5)	12(4)	-31(5)
C(25)	43(5)	47(5)	28(5)	-4(4)	-8(4)	-9(4)
C(26)	47(6)	51(6)	35(5)	3(4)	-10(4)	-15(5)
C(27)	63(3)	84(4)	83(4)	2(3)	-23(3)	-33(3)
C(28)	47(5)	49(6)	34(5)	4(4)	-16(4)	-12(4)
C(29)	40(5)	46(5)	28(5)	0(4)	-8(4)	-7(4)

C(30)	37(5)	52(6)	38(5)	-3(4)	-4(4)	-11(4)
C(31)	63(3)	84(4)	83(4)	2(3)	-23(3)	-33(3)
C(32)	63(3)	84(4)	83(4)	2(3)	-23(3)	-33(3)
C(33)	63(3)	84(4)	83(4)	2(3)	-23(3)	-33(3)
C(34)	63(3)	84(4)	83(4)	2(3)	-23(3)	-33(3)
C(35)	45(5)	55(6)	36(5)	8(4)	-6(4)	-14(5)
C(36)	86(9)	79(9)	65(8)	14(7)	-6(7)	-43(7)
C(37)	58(7)	84(9)	57(8)	3(6)	10(6)	-7(6)
C(38)	56(7)	88(8)	40(6)	20(6)	-9(5)	-14(6)

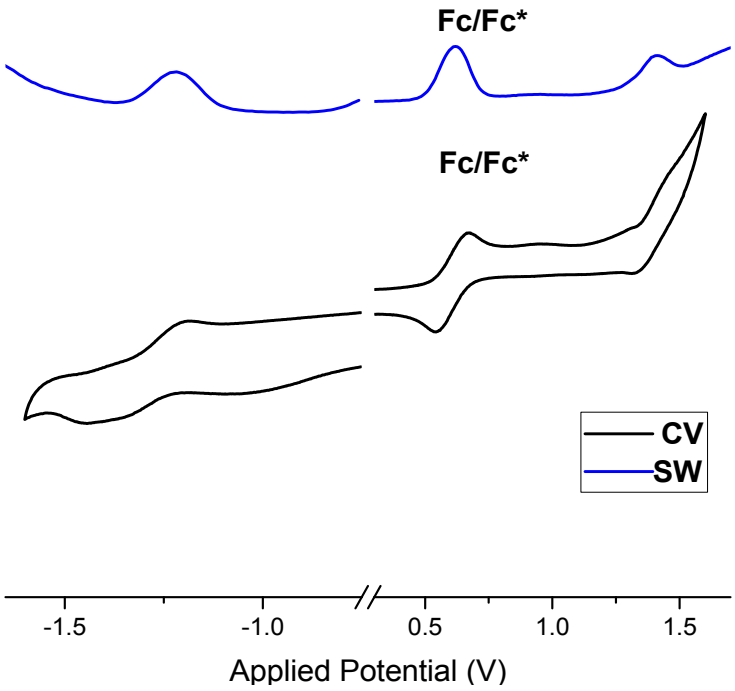

Figure S6. Cyclic (CV) and square wave (SW) voltammograms of Pd-por in THF.

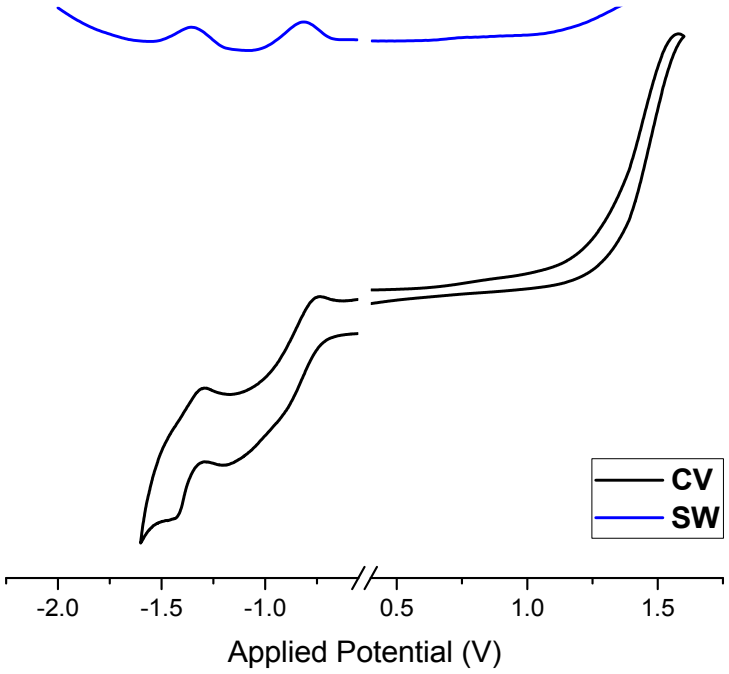

Figure S7. Cyclic (CV) and square wave (SW) voltammograms of Sn-por in THF.

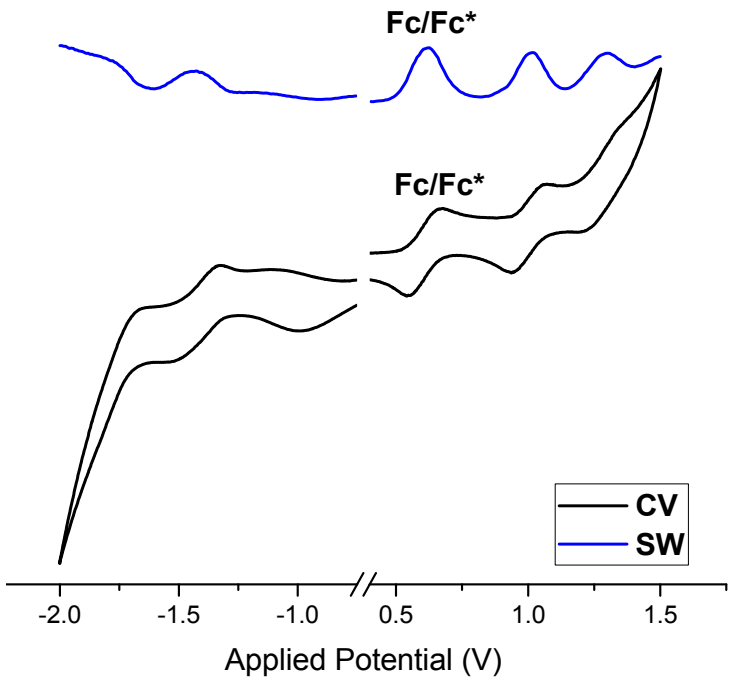

Figure S8 Cyclic (CV) and square wave (SW) voltammograms of Zn-por in THF.

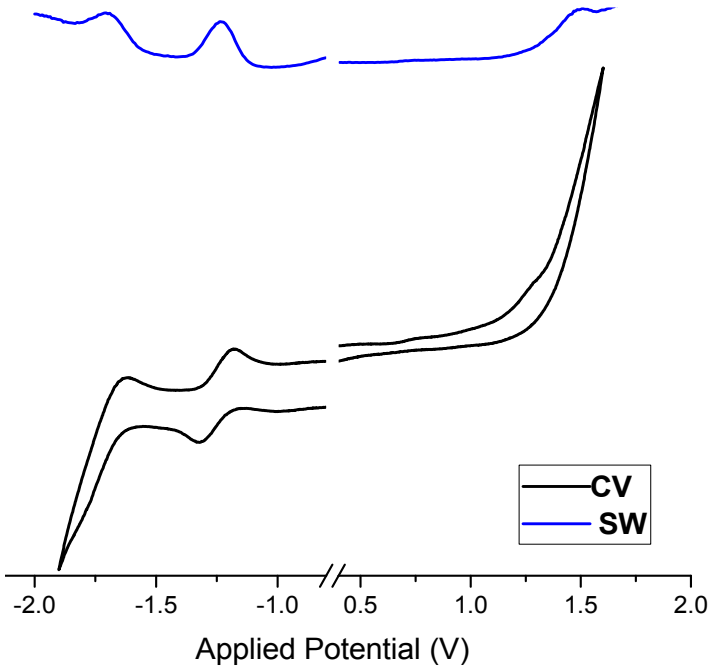

Figure S9. Cyclic (CV) and square wave (SW) voltammograms of Pt-por in THF.

Table S5. Electrochemical redox data of Zn-por, Sn-por, Pt-por, and Pd-por in THF. All potentials are reported *vs*. SCE. Ferrocene/ferrocenium^{+} redox couple was used as internal standard ($E_{1/2ox}$ observed at 0.65 V).

Compound	Red 1	Red 2	Ox 1	Ox 2
Pd-por	-1.19 V	-	1.43 V	-
Pt-por	-1.24 V	-1.70 V	1.53 V	-
Sn-por	-0.79 V	-1.33 V	-	-
Zn-por	-1.41 V	-	1.04 V	1.31 V

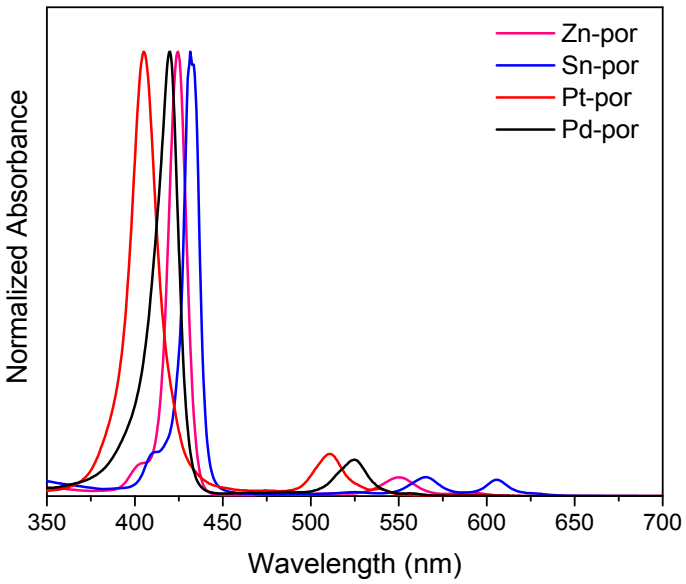

Figure S10. Absorption spectra of Zn-por, Sn-por, Pt-por, and Pd-por in toluene at room temperature.

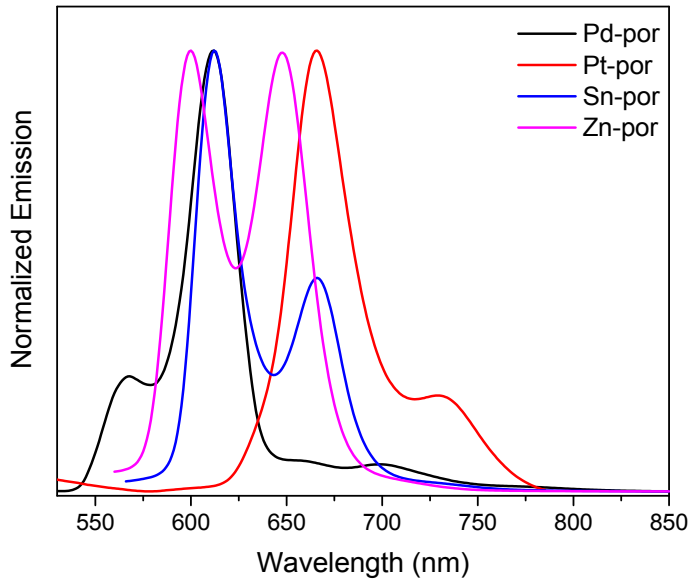

Figure S11. Emission spectra of Zn-por, Sn-por, Pt-por, and Pd-por in toluene at room temperature upon excitation at 549, 556, 510, and 524 nm, respectively.

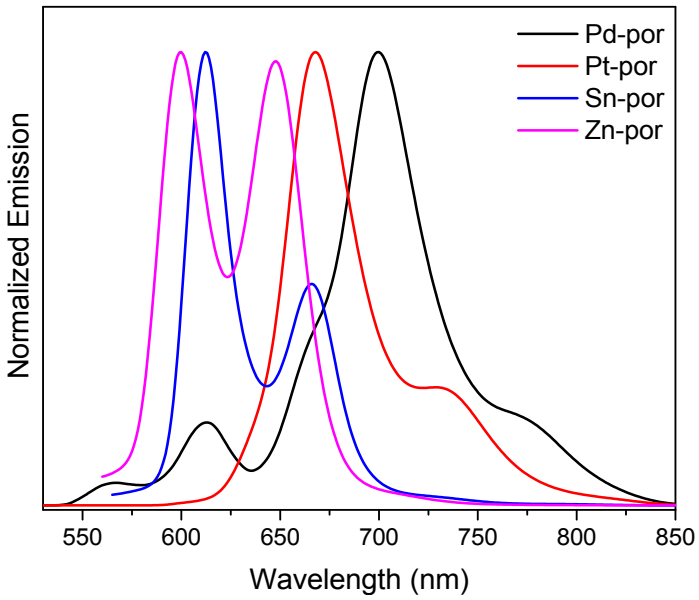

Figure S12. Emission spectra of Zn-por, Sn-por, Pt-por, and Pd-por in degassed toluene at room temperature upon excitation at 549, 556, 510 and 524 nm respectively.

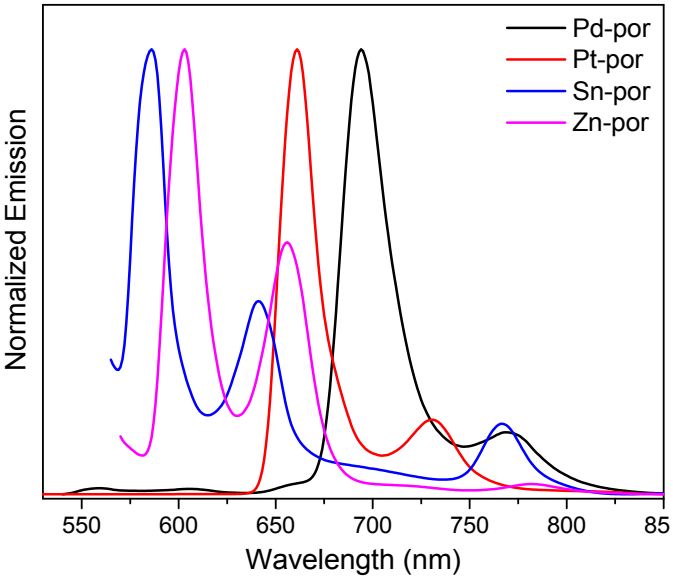

Figure S13. Emission spectra of Zn-por, Sn-por, Pt-por, and Pd-por in toluene glass at 77 K upon excitation at 549, 556, 510 and 524 nm respectively.

Table S6. Emission data for Zn-por, Sn-por, Pt-por and Pd-por in toluene.

Compound	Absorption	Emission (77 K)	Emission (r.t.)				
	λ_{max}/nm (ε/mM^{-1} cm^{-1})	λ_{max} (nm)	λ_{max} (nm)	Φ_{fluo} (%)	Φ_{phos} (%)	τ_{fluo}	τ_{phos}
Zn-por	425 (496.9) 550 (22.1) 590 (5.0)	603, 656, 783[a]	599, 646	3.8 3.8[b]		1.9 ns 2.3ns[b]	
Sn-por	432 (502.7) 565 (16.9) 605(14.5)	608, 663, 789[a]	612, 667	1.2 1.2[b]		< 1 ns < 1 ns[b]	
Pd-por	420 (341.2) 525 (28.2)	558, 605, 694,[a] 769[a]	565, 612, 698[a] 567,[b] 613,[b] 701,[a,b] 778[a,b]	0.047 0.03[b]	0.0013 0.3[b]	< 1 ns < 1 ns[b]	604 ns 9 µs[b]
Pt-por	405 (193.4) 511 (18.8)	661,[a] 731[a]	666,[a] 730[a]		0.095 3[b]		681 ns 6 µs[b]

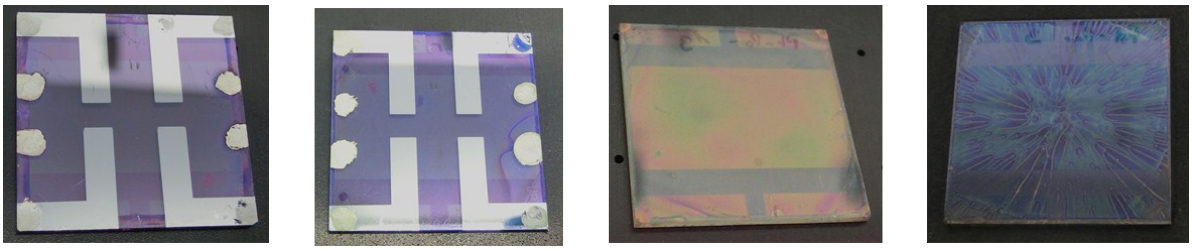

Figure S14. Exemplary of pictures of thin films prepared with Zn-por (left), Sn-por (middle left), Pt-por (middle right) and Pd-por (right).

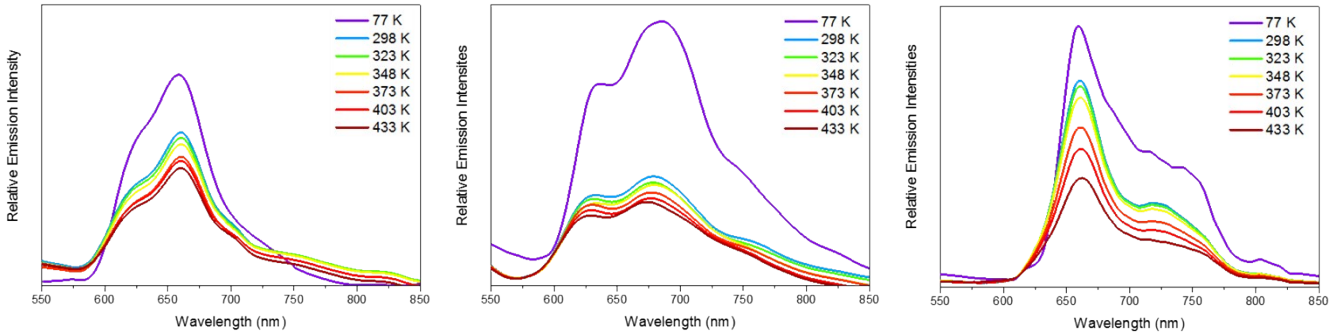

Figure S15. Emission spectra of Zn-por (left), Sn-por (middle), and Pt-por (right) films upon applying different temperatures.

Table S7. Vertical excitation energies (ΔE in eV), oscillator strengths and character of the states (in terms of the most significant singlet excitation contributions) for the four lowest-lying singlet state (Q and Soret (So)-like bands) calculated using TDDFT theory (B3LYP/def2-TZVP//B3LYP/def2-TZVP).

State	ΔE (eV)	*f*	Character
S_1	2.21	0.014	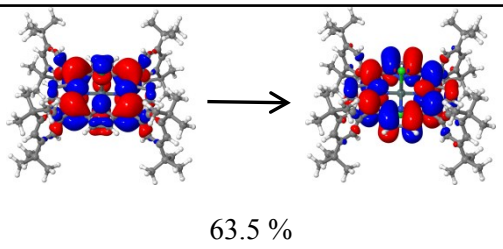 63.5 % 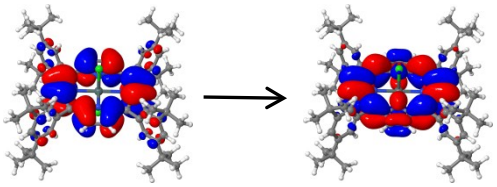 35.8%
S_2	2.21	0.013	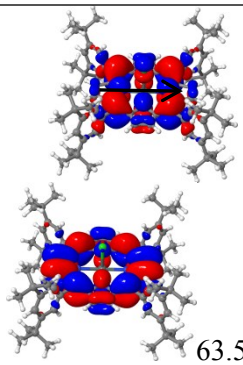 63.5 % 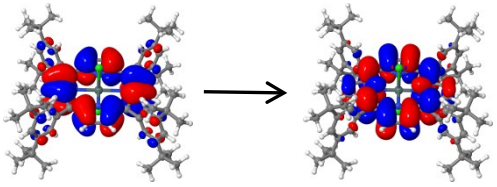 35.8%
S_3	3.04	0.867	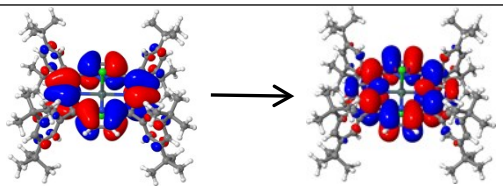 56.5% 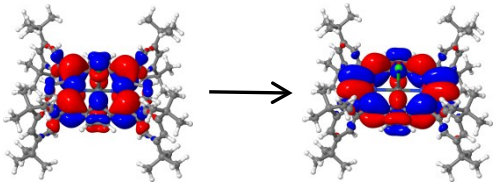 29.4%

S_4	3.04	<0.867	 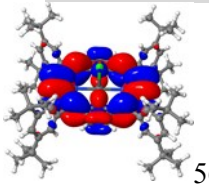 56.6 % 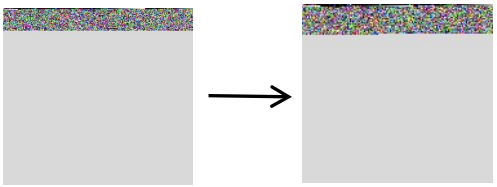 29.4 %

Table S8. Vertical excitation energies (ΔE in eV), oscillator strengths and character of the states (in terms of the most significant singlet excitation contributions) for the four lowest-lying triplet states computed using TDDFT theory (B3LYP/def2-TZVP//B3LYP/def2-TZVP).

State	ΔE (eV)	*f*	Character
T_1	1.53	0.000	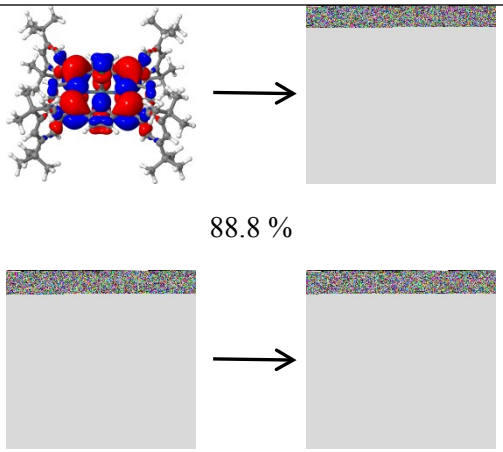 88.8 % 9.0 %
T_2	1.53	0.000	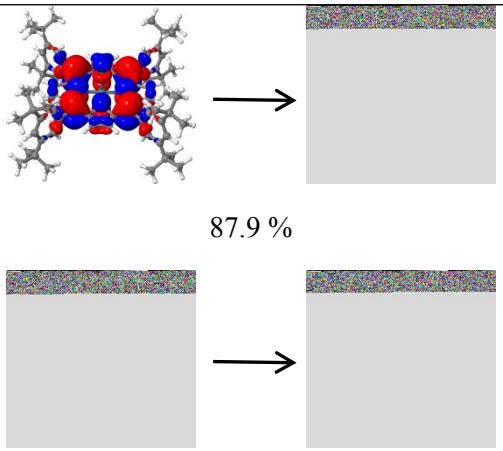 87.9 % 9.0 %
T_3	1.98	0.000	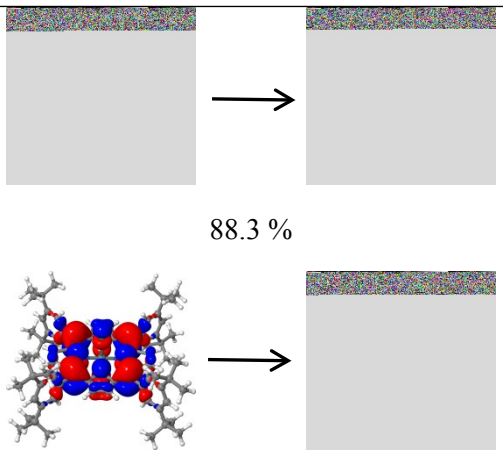 88.3 %

			10 %
T_4	1.98	0.000	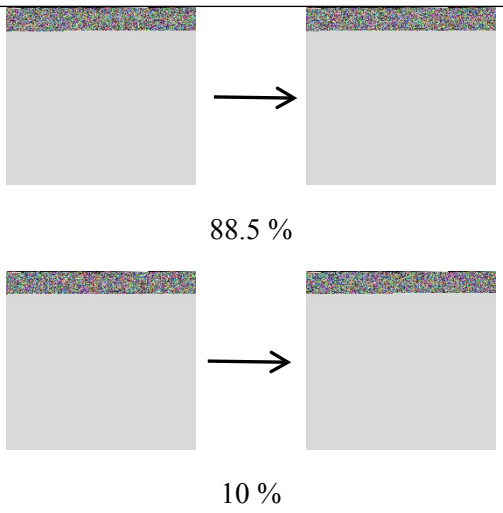

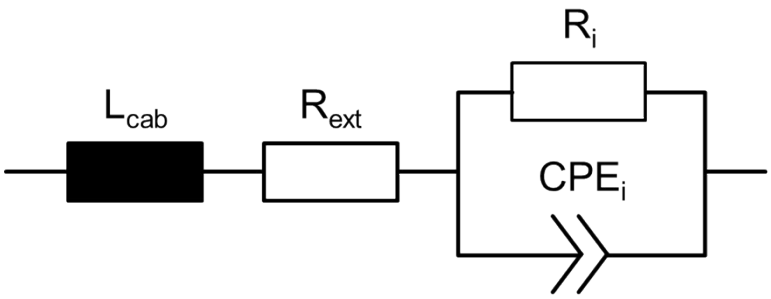

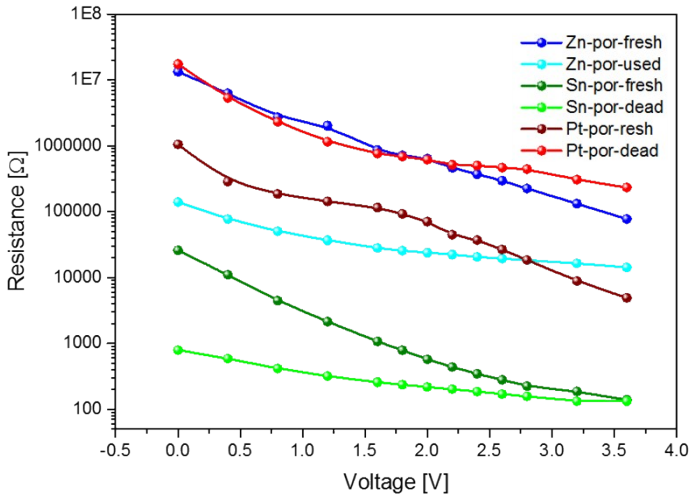

Figure S16. Upper part – Electrical circuit model used for the EIS fittings. Lower part – Changes in the resistance measured at different applied voltages for fresh and dead Zn-por, Pt-por, and Sn-por devices.

5. Cartesian coordinates (bohr)

N	-0.00070163947962	-3.98524147743371	-0.00249598938222
N	0.00021246120007	3.98462745442786	-0.00153515775168
N	3.98287161052874	-0.00066036589201	-0.00301803855403
N	-3.98308815150421	0.00026774236503	-0.00221612367617
C	2.11260735161694	-5.47564000422855	-0.00060579701344
C	-2.11306386841431	5.47507470172744	0.00050342807448
C	-2.11437025105273	-5.47515883572419	-0.00108831942387
C	2.11383935462672	5.47452684975690	-0.00031373066852
C	4.63682118956045	-4.63902088861163	-0.00058455224290
C	-4.63734249230257	4.63867940131832	0.00038699731064
C	-4.63843012873573	-4.63796848271252	-0.00134366657428
C	4.63793065315117	4.63754268094888	-0.00122005954424
C	5.47237735800930	-2.11420130686939	-0.00141218366406
C	-5.47269305372294	2.11390228357990	-0.00052554290180
C	-5.47321029899097	-2.11295366340718	-0.00147238788620
C	5.47288877966167	2.11257953820613	-0.00189338895804
C	1.28451715760560	-8.06901346843259	0.00165194624263
C	-1.28502153462360	8.06847132169763	0.00286933859572
C	-1.28690922324771	-8.06877224069051	0.00128010222747
C	1.28641901509266	8.06806234330194	0.00232404214106
C	6.64657771990485	-6.63805034846878	0.00035844709385
C	-6.64671319654181	6.63793206227444	0.00109366399720
C	-6.64826614213066	-6.63690683161214	-0.00100635066907
C	6.64772416616752	6.63645812626291	-0.00095167644265
C	8.06602841319969	-1.28666406361755	0.00022853188354
C	-8.06632135870079	1.28636365014330	0.00088724103810
C	-8.06657938919758	-1.28480712922493	0.00023038729107
C	8.06637190787191	1.28446954748044	-0.00016738409461
C	7.59166982355192	-7.56717167430311	2.27185610645211
C	-7.59198529820867	7.56737632434063	2.27221953682958
C	-7.59375337831060	-7.56624223849906	-2.27228430214948
C	7.59345237949666	7.56539379790970	-2.27230945583532
C	-7.59264085655113	7.56708964611882	-2.27010025980002
C	7.59319516702269	-7.56668601165674	-2.27076490652627
C	7.59322360182760	7.56589266695080	2.27017695478783
C	-7.59382784001403	-7.56627632086010	2.27018129782854
C	9.47663534874718	-9.41328642133992	2.31706108876543
C	-9.47612728303994	9.41438111477082	2.31738903480368
C	-9.47737330676561	-9.41375655369489	-2.31730455102348
C	9.47709669875183	9.41291871822754	-2.31733124817663
C	-9.47671800790986	9.41412156275884	-2.31497376215982
C	9.47787375295667	-9.41305516191078	-2.31530461855459
C	9.47714641156868	9.41310797776381	2.31502864122990
C	-9.47763602757097	-9.41361074433533	2.31508349378892
C	10.38387029031889	-10.30117847691673	0.00107648951397
C	-10.38253924289045	10.30269911293914	0.00121436853054
C	-10.38324886131109	-10.30251385028890	-0.00114466531337
C	10.38287965102990	10.30187632181001	-0.00123637521921
SN	-0.00016333953503	-0.00028255759326	-0.00287410825749
H	2.52322171926020	-9.68383823446611	0.00333414816150
H	-2.52353310855866	9.68343662731410	0.00474040756062
H	-2.52595252668009	-9.68333221133401	0.00271238522435
H	2.52538812876551	9.68267897968681	0.00374535253302
H	9.68061491505128	-2.52561517085621	0.00167387703210
H	-9.68102744065348	2.52511040375461	0.00234803126974
H	-9.68162962486822	-2.52317163153489	0.00109085895998
H	9.68125534187844	2.52300385565824	0.00104074163529

H	6.83053536336253	-6.81745264601134	4.01663099778309
H	-6.83161626917762	6.81728320193101	4.01729570137076
H	-6.83363094952124	-6.81581983590689	-4.01722840432548
H	6.83351680398256	6.81481678844967	-4.01718495293690
H	-6.83265674108057	6.81683427755333	-4.01516621137054
H	6.83324398168234	-6.81650969173875	-4.01581808978766
H	6.83304829640701	6.81581323771188	4.01523097935459
H	-6.83372691429119	-6.81605300849950	4.01523622747703
C	10.47414391393302	-10.38194014838691	4.86923979418746
C	-10.47372930935257	10.38316124893077	4.86934273045630
C	-10.47460672745485	-10.38318503570693	-4.86927195320441
C	10.47420609514312	10.38211381069296	-4.86946963817998
C	-10.47456468009059	10.38298253760640	-4.86687521262092
C	10.47606934658261	-10.38192252360383	-4.86719118535586
C	10.47445404014877	10.38243488852765	4.86701193767702
C	-10.47510736256386	-10.38299515512922	4.86696942994033
H	11.84045600437893	-11.72500727097110	0.00149991829898
H	-11.83854171947198	11.72715651053937	0.00138572479966
H	-11.83857509785944	-11.72764265922036	-0.00116212910316
H	11.83812809374197	11.72707877956242	-0.00129761046781
C	-12.53880853124662	12.40152594433989	4.56989405429346
C	-11.59857674901889	8.15440008224034	6.37812212155504
C	-8.27611865216368	11.55356162778597	6.38873175044368
C	-12.54021514189460	12.40069449459210	-4.56683781261697
C	-8.27721140764945	11.55422227541533	-6.38603913165288
C	-11.59866199975494	8.15428179463915	-6.37632941359105
C	-12.54144987118980	-12.40004141746163	4.56715401806019
C	-8.27739158963005	-11.55512121714033	6.38495322788433
C	-11.59835252826107	-8.15461045526761	6.37749669700621
C	-12.53940227877310	-12.40181953542541	-4.56950738607518
C	-11.59959676493077	-8.15503871021593	-6.37886750013747
C	-8.27650275166175	-11.55340625109762	-6.38816223271210
H	-8.95556026762578	-12.23838192923429	8.21239184473160
H	-7.44813745972783	-13.15215872534067	5.37322779282770
H	-6.77817318994393	-10.18644913005253	6.74188942882121
H	-13.17756961608863	-13.01309108044772	6.43219565712129
H	-14.19007625453810	-11.67425536230597	3.55934720092630
H	-11.85358897737809	-14.07023875118560	3.56834819132725
H	-12.30079949662288	-8.81220122827128	8.20516552969338
H	-10.19613469358174	-6.68668252797666	6.73379307660606
H	-13.17378912719699	-7.29106509325469	5.36054263172290
H	-8.95470560637054	-12.23606217007110	-8.21579734694678
H	-6.77810226004768	-10.18377518607822	-6.74482926547159
H	-7.44621930090806	-13.15051913734200	-5.37737569267112
H	-12.30323826953644	-8.81266117044916	-8.20607425270821
H	-13.17441289914316	-7.29184314836462	-5.36065082548125
H	-10.19791410697816	-6.68680237673889	-6.73608233714050
H	-13.17469866109547	-13.01575538256188	-6.43455149593988
H	-11.85028791113022	-14.07124101330544	-3.57027292986658
H	-14.18874534521381	-11.67725830497154	-3.56200085588017
H	-12.30127560452664	8.81108575013856	8.20602078468874
H	-13.17404108967067	7.29235672793918	5.35995020562231
H	-10.19717634690463	6.68550407991765	6.73376805937491
H	-8.95421470817413	12.23354702358971	8.21742094356867
H	-6.77615878876346	10.18504113844454	6.74316237524516
H	-7.44793522700327	13.15270706082416	5.37944664539639
H	-13.17408129963262	13.01512963447152	6.43504989551948
H	-11.84992689310403	14.07120577294883	3.57092297893673
H	-14.18815586437046	11.67691644321083	3.56243839197872

H	-8.95570937511837	12.23557378980608	-8.21406426002078
H	-7.44831771837982	13.15239034808572	-5.37579079964764
H	-6.77764358526096	10.18565928823101	-6.74201286725672
H	-13.17535597115181	13.01504505186527	-6.43179790516713
H	-14.18949194724634	11.67517211766489	-3.55990751042665
H	-11.85195992757590	14.07006636163616	-3.56691635234159
H	-12.30298759931694	8.81155677246685	-8.20340783085934
H	-10.19630543583571	6.68674059284520	-6.73384751248497
H	-13.17284829464784	7.29027930331204	-5.35783748697802
C	12.54111676226671	12.39914239676537	4.56729696105551
C	8.27665680718282	11.55480471564501	6.38470203664827
C	11.59723649003632	8.15392125040106	6.37774703926141
C	12.53934848017651	12.40041557729652	-4.56994503870356
C	11.59866575651174	8.15372662604294	-6.37912843028323
C	8.27607276934382	11.55266543630595	-6.38806757490046
H	8.95454308929916	12.23768205423424	8.21237869443270
H	7.44783748097115	13.15212794710097	5.37303028599070
H	6.77715885993929	10.18633954646776	6.74126585653848
H	13.17707691198992	13.01234359739001	6.43235023337903
H	14.18967455782485	11.67294932417369	3.55968268078517
H	11.85362308897321	14.06928144501750	3.56815855614405
H	12.29964423574564	8.81151095816035	8.20543683218263
H	10.19476047179774	6.68627594084123	6.73400888269138
H	13.17253733642248	7.29002917313486	5.36090695852928
H	13.17462312144031	13.01415955293319	-6.43504819975248
H	11.85055258890612	14.07001835390490	-3.57078081382624
H	14.18862960386726	11.67562112682572	-3.56251928782133
H	12.30181644276144	8.81112148051187	-8.20660550798239
H	13.17372535238961	7.29064549165414	-5.36123778049571
H	10.19686335801292	6.68550112770530	-6.73575815086660
H	8.95387776570772	12.23445652354431	-8.21617216194448
H	6.77694792470190	10.18356022141778	-6.74373178795271
H	7.44681795232264	13.15051171116591	-5.37758571204587
C	12.54216615230042	-12.39915841136058	-4.56697199657451
C	8.27893280220439	-11.55402525621510	-6.38608008776002
C	11.59948679255307	-8.15295785958513	-6.37685287751628
C	12.53982641888350	-12.39969712636067	4.56995132707163
C	11.59808909009594	-8.15299462459860	6.37846565309861
C	8.27647709186683	-11.55293769772203	6.38809032719433
H	13.17667452727102	-13.01439677179538	-6.43183100187722
H	14.19168203111804	-11.67289937906347	-3.56098561894322
H	11.85436252715390	-14.06810179733609	-3.56602992264628
H	8.95716493512271	-12.23413740715532	-8.21465987203578
H	7.45162029590967	-13.15322412315242	-5.37617210766149
H	6.77824724436938	-10.18642955925507	-6.74076346864832
H	12.30536095488207	-8.81037721322051	-8.20326528281415
H	10.19632175713648	-6.68658762938229	-6.73574140749611
H	13.17245480497481	-7.28746875729622	-5.35777316791309
H	8.95418433658652	-12.23221839884724	8.21716690656518
H	6.77591301047231	-10.18493399511251	6.74163725915987
H	7.44925620489535	-13.15257369550745	5.37881146947181
H	13.17460872306300	-13.01365840487032	6.43512766902431
H	11.85166262190496	-14.06922218487765	3.57023486737216
H	14.18927375001281	-11.67423597703818	3.56328734612733
H	12.30136874976136	-8.80995987121482	8.20602444513045
H	13.17301046297584	-7.28984933548205	5.36041724469802
H	10.19600362578401	-6.68497373891015	6.73476749712668
Cl	-0.00090082403867	0.00061188172489	-4.67805752969036
Cl	0.00010699116096	-0.00069472153564	4.67285886686425

References

1 G. Di Carlo, A. Orbelli Biroli, M. Pizzotti, F. Tessore, V. Trifiletti, R. Ruffo, A. Abbotto, A. Amat, F. De Angelis and P. R. Mussini, *Chem. - A Eur. J.*, 2013, **19**, 10723.

2 M. J. Crossley, P. Thordarson and R. A.-S. S. Wu, *J. Chem. Soc. Perkin Trans. 1*, 2001, 2294.

3 G. A. Crosby and J. N. Demas, *J. Phys. Chem.*, 1971, **75**, 991.

4 P. G. Seybold and M. Gouterman, *J. Mol. Spectrosc.*, 1969, **31**, 1.

5 P. A. M. Dirac, *Proc. Royal Soc. A*, 1929,**123**, 714.

6 J. C. Slater, *Phys. Rev.*, 1951, **81**, 385.

7 S. H. Vosko, L. Wilk, M. Nusair, *Can. J. Phys.*, 1980, **58**, 1200.

8 A. D. Becke, *Phys. Rev. A*, 1988, **38**, 3098.

9 C. Lee, W. Yang, R. G. Parr, *Phys. Rev. B*, 1988, **37**, 785.

10 A. D. Becke, *J. Chem. Phys.*, 1993, **98**, 5648.

11 F. Weigend, R. Ahlrichs, *Phys. Chem. Chem. Phys*., 2005, **7**, 3297.

12 B. Metz, H. Stoll, M. Dolg, *J. Chem. Phys.*, 2000, **113**, 2563.

13 TURBOMOLE V7.0 2015, a development of University of Karlsruhe and Forschungszentrum Karlsruhe GmbH, 1989-2007, TURBOMOLE GmbH, since 2007; available from http://www.turbomole.com.